Optical Continuous Variable Squeezed Light

Edy Alberto Flores Leal[1]

[1]KTH Royal Institute of Technology, Stockholm, Sweden

Abstract. We observed the dependence of the Second Harmonic Generation (SHG) power to the temperature with an experimental optimal phase matching temperature of $T_0 \sim 40.54\ ^\circ\mathrm{C}$. Also, we registered a maximum level of squeezing and anti-squeezing of 0.21 dB and 0.28 dB, respectively, which implied the domination of anti-squeezing effects. We used a periodically poled Lithium Niobate (ppLN) waveguide for SHG, converting the 1550 nm fundamental laser light into 775 nm. A second ppLN waveguide facilitated spontaneous parametric down-conversion, generating squeezed light at 1550 nm. Temperature controllers were used to optimize the phase-matching conditions in both waveguides, enhancing nonlinear interactions.

1. Introduction

The study of states of light has led to the development of new technologies and several other discoveries in Physics. In particular, squeezed states of light have proven essential to quantum communications, quantum metrology, detection of gravitational waves, and more [1, 2, 3]. The physical principle consists of "squeezing" one of the canonical variables in exchange for increasing the uncertainty of the other one. There are two types of squeezing: Discrete Variable (DV) and Continuous Variable (CV) Squeezing. The main difference between them is the size of their Hilbert Space; for instance, DV Squeezing would have a finite Hilbert space characterized by discrete quantum numbers, while CV Squeezing has an infinite Hilbert space associated with the canonical variables of position and momentum [4].

The production of optically squeezed states of light requires Periodically Polarized (PP) crystals with a highly nonlinear refractive nature. Normally, in linear optics, the polarization is described in terms of the rapidly changing electric field $\tilde{E}(t)$ and susceptibility χ. In nonlinear materials, the polarization is expanded in powers of the electric field such that

$$\tilde{P}(t) = \epsilon_0 \sum_{n=1} \chi^{(n)} \tilde{E}^n(t) = \sum_{n=1} \tilde{P}^{(n)}(t), \tag{1}$$

where ϵ_0 is the permittivity of free space [5]. One alternative to produce squeezing is using materials like periodically poled Lithium Niobate $\mathrm{LiNbO_3}$ (ppLN), which for the $\chi^{(2)}$ term cannot be neglected. If we consider a monochromatic electric field

$$\tilde{E}(t) = E\mathrm{e}^{-\mathrm{i}\omega t} + \text{c.c.}, \tag{2}$$

where E is a complex amplitude, ω is the angular frequency, and t is the time, the second-order polarization is

$$\tilde{P}^{(2)}(t) = 2\varepsilon_0 E E^* + \left(\varepsilon_0 \chi^{(2)} E^2 \mathrm{e}^{-2\mathrm{i}\omega t} + \text{c.c.}\right). \tag{3}$$

From Eq. (3), we notice that, in a material with susceptibility $\chi^{(2)}$, the polarization consists of a zero frequency term ($2\varepsilon_0 E E^*$) that represents a static electric polarization called optical rectification, and a 2ω frequency term ($\varepsilon_0 \chi^{(2)} E^2 \mathrm{e}^{-2\mathrm{i}\omega t}$ + c.c.) that produces radiation at this second-harmonic frequency [5, 6]. This yields the Second Harmonic Generation (SHG).

In this report, we studied the SHG dependence on the temperature and how such dependence follows a particular function given the conditions of the experiment. Furthermore, we analyzed the squeezing and anti-squeezing in an experimental setup. Finally, we contrasted the experimental results with the theoretical expectations to determine the dominance of squeezing or anti-squeezing effects.

2. Experiment

2.1. Characterization of the SHG

The SHG characterization represents an essential part of the description of second-order nonlinear susceptibility processes. The SHG process occurs in non-centrosymmetric materials (such as Lithium Niobate), which lack inversion symmetry. This property enables three-wave mixing, where two photons of the same fundamental frequency ω interact through the nonlinear medium to generate a photon at twice the frequency, 2ω, in what is called up-conversion. Efficient SHG requires the conservation of momentum, which is expressed through the phase mismatch $\Delta k = 2k_\omega - k_{2\omega}$. When $\Delta k = 0$, the fundamental and second harmonic waves remain in phase as they propagate. However, when $\Delta k \neq 0$, the two waves gradually fall out of phase, limiting SHG efficiency. The distance over which the waves become completely out of phase is called the coherence length, defined as $L_{\mathrm{coh}} = 2/\Delta k$. Under perfect phase-matching conditions (implying conservation of momentum), the second harmonic power corresponds to

$$P_{\mathrm{SHG}} = P_{\mathrm{in}} \tanh^2(\sqrt{\alpha_{\mathrm{SHG}} P_{\mathrm{in}}}). \tag{4}$$

This result is achieved by the Quasi-Phase Matching (QPM), a technique that periodically inverts the sign of $\chi^{(2)}$ within the nonlinear crystal in a process known as periodic poling [6, 7]. By flipping the nonlinear coefficient every coherence length, QPM compensates for the phase mismatch. Since it is not always possible to satisfy the condition $\Delta k = 0$, instead, a different expres-

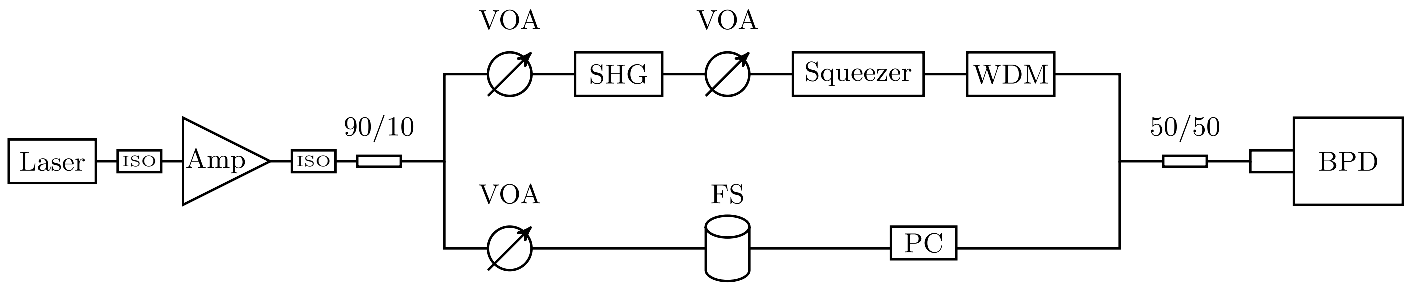

Figure 1: **Schematic diagram of the squeezing experiment**. The laser is a Single Frequency Distributed (SFD) feedback fiber laser with an emission centered at 1550 nm. ISO: Isolator; VOA: Variable Optical Attenuators; SHG: Second Harmonic Generator; FS: Fiber Stretcher; WDM: Wavelength Division Multiplexing; PC: Polarization Controller; BPD: Balanced Photo Detector.

sion for $P_{\rm SHG}$ is obtained:

$$P_{\rm SHG} \propto P_{\rm in} L^2 {\rm sinc}^2 \left(\frac{\Delta k L}{2\pi} \right). \quad (5)$$

where $P_{\rm SHG}$ is the power of the SHG light, $P_{\rm in}$ is, for this experiment, the input 1550 nm light, Δk is the difference between wave vectors, and L is the length of the waveguide.

2.2. Experimental setup

Figure 1 shows the schematic of the experimental setup used for the squeezing. The setup consisted of several parts, the first being a single-frequency distributed feedback (DFB) fiber laser at 1550 nm, amplified by a low-noise fiber amplifier. This laser system also had a $90:10$ fiber coupler, which directed 90% of the light to the nonlinear waveguide chain and reserved the remaining 10% for the Local Oscillator (LO), both using Variable Optical Attenuators (VOA) to regulate the optical power.

The second part of the setup was a SHG that used a ppLN waveguide to convert the 1550 nm input into 775 nm. The 775 nm light was then transferred to a second ppLN waveguide and produced the squeezed light at 1550 nm via spontaneous parametric down-conversion. A Wavelength Division Multiplexer (WDM) was also employed to remove residual 775 nm light to prevent added shot noise in the LO, while temperature controllers optimized the phase-matching conditions for both waveguides.

The third part of the setup used an LO consisting of a Fiber Stretcher (FS) that adjusted the path length and phase of the LO light. This part also involved a Polarization Controller (PC) that matched the LO light polarization to the squeezed states to maximize the squeezing. Finally, the fourth part of the setup was an AC-coupled, high-speed dual-balanced InGaAs photodiode that operates between 300kHz and 1GHz. It was possible to perform the experiment at room temperature since we worked within the Continuous Variable (CV) regime.

2.3. Experimental methods

We first measured the fundamental optical power entering the SHG waveguide. As is known, quantum correlations are susceptible to several perturbative processes. Disruptive processes such as random scattering of photons or absorption could lead to decoherence or loss. Thus, we employed an Integrating Sphere (IS) whose geometry and surface coating helped to distribute the scattering homogeneously in all directions [8]. The stability of the optical power over five minutes was recorded and analyzed.

The second part of the experiment consisted of the analysis of the temperature dependence of the SHG efficiency. Increments of $2°$C were performed, starting from $25°$C until $53°$C, and then the optical power was measured. The measurements let us determine the optimal phase-matching temperature based on Eq. (4).

The third and final part of the experiment involved the analysis of dark and shot noise, two noise sources that affect the accuracy of the measurements. Dark noise originates from a dark current and it is produced by thermal energy that generates charges produced in the detector [9]. Shot noise appears from the discrete nature of the electric charge, which causes random fluctuations in current due to the random arrival of individual charge carriers [10]. Squeezing and anti-squeezing levels were optimized by tuning the LO polarization. We determined the maximum squeezing level by comparing the shot noise with the peaks and valleys of the sinusoidal-like arches plotted in the laboratory.

3. Results

3.1. Characterization of the SHG

The SHG characterization had two parts. The first one, as described in the previous section, consisted of the fundamental optical power measurement. We summarized the statistics retrieved from the experiment in Table 1.

Table 1: Statistics of the fundamental optical power measurements in a period of ~ 5 minutes

Minimum	Maximum	Mean	Std. Dev.
578.82 mW	595.19 mW	588.08 mW	4.13 mW

A total of 95704 samples were counted. The maximum and minimum optical powers retrieved were 595.19 mW and 578.82 mW, respectively, with a difference of 16.37 mW. The standard deviation was 4.13 mW with a 588.08 mW optical power mean. The second part of the SHG characterization consisted of the observation of its dependence on the temperature.

Figure 2 shows the experimental results and the fitting curve:

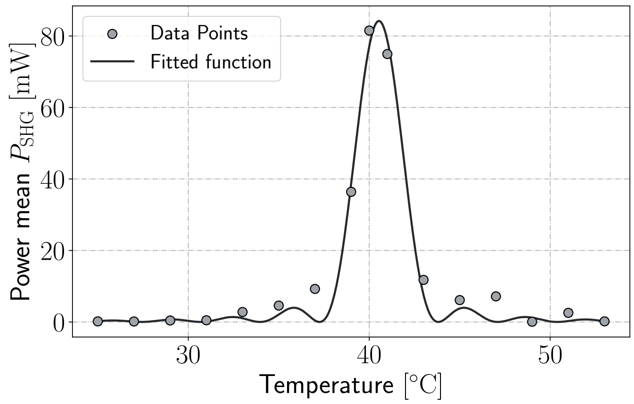

Figure 2: **Plot of the temperature T [°C] versus the power mean** P_{SHG} [mW]. The points represent the experimental data and the solid line represents the curve fitted.

To make the fit, we used a relation based on Eq. (4). Both length and refractive index of the waveguide depend on the temperature, so using $\Delta kL = b(T - T_0)$ led to the Eq.

$$P_{\mathrm{SHG}} \propto P_{\mathrm{in}} A \mathrm{sinc}^2[b(T - T_0)], \quad (6)$$

where A and b are arbitrary constants, T is the temperature, and T_0 the optimal phase matching temperature. We provided the initial guesses of $A = 0.15$, $b = 1\,°\mathrm{C}^{-1}$, and $T_0 = 40\,°\mathrm{C}$ based on the position of the data points and used the mean power from the fundamental optical power measurements. The experimental result gave an optimal phase matching temperature of $T_0 \sim 40.54\,°\mathrm{C}$, while the experimental SHG efficiency was $P_{\mathrm{SHG}} \sim 81.53 \pm 0.16$ mW. The fit parameters are presented in Table 2:

Table 2: Fit parameters of the SHG Characterization dependence on the temperature

A	b	T_0
0.14	$0.96\,°\mathrm{C}^{-1}$	$40.54\,°\mathrm{C}$

3.2. Squeezing measurement

After studying the temperature dependence of the SHG Characterization, we measured the dark and shot noise in the experiment. Both measured values are expressed in dBm units and are found in Table 3:

Table 3: Experimental values of the dark and shot noises

Dark noise	**Shot noise**
−98.09 dBm	−97.37 dBm

A dark noise of −98.09 dBm was seen in the experiment, while the shot noise recorded −97.37 dBm. The difference between the dark and shot noise is 0.72 dBm. A total of five sets of peaks and valleys of different squeezing arches were measured by a single sweep measurement. The values of these points are found in Table 4:

Table 4: Experimental valleys and peaks of the squeezing arches. SQ stands for Squeezing, and ASQ stands for Anti-squeezing

Valley [dBm]	**SQ** [dB]	**Peak** [dBm]	**ASQ** [dB]
−97.58	0.21	−97.11	0.26
−97.53	0.16	−97.09	0.28
−97.51	0.14	−97.11	0.26
−97.55	0.18	−97.11	0.26
−97.53	0.16	−97.09	0.28

Using the values on Table 4, the squeezing and anti-squeezing were measured. To compute the experimental squeezing, we calculated the (absolute) difference between each valley and the shot noise. For the anti-squeezing, we subtracted the shot noise from the peak. The highest squeezing level had a value of 0.21 dB, while the highest anti-squeezing level obtained was 0.28 dB.

4. Discussion

As discussed in the previous section, the mean fundamental optical power recorded was 588.08 mW with a standard deviation of 4.13 mW. The stability of the power over the 5-minute time scale was linked to the coefficient of variation or Relative Standard Deviation (RSD). For this case, the RSD was

$$\mathrm{RSD} = \frac{\sigma}{\mu} \times 100\% \approx 0.702\%. \quad (7)$$

A small RSD value indicated that the power outcome was stable during the 5-minute measurements. Regarding the SHG characterization, the experimental curve showed the $\mathrm{sinc}^2(x)$ expected from the not-perfect QPM, a consequence of the output wave getting out of phase with its driving polarization [5]. The experiment yielded an optimal phase matching temperature of $T_0 \sim 40.54\,°\mathrm{C}$, while the experimental SHG power at T_0 was $P_{\mathrm{SHG}} \sim 81.53 \pm 0.16$ mW.

For the third part of the experiment, we first measured a dark and shot noise of −98.09 dBm and −97.37 dBm. More importantly, a maximum value for squeezing and anti-squeezing was experimentally found, in particular, 0.21 dB and 0.28 dB, which implies a more significant anti-squeezing effect contrasted to the squeezing effect. To compare with theoretical results, we computed the expected levels of squeezing and anti-squeezing. First, we obtained the squeezing parameter R in the following fashion:

$$R = \sqrt{\alpha_{\mathrm{OPA}} P_{\mathrm{SHG}}(T_0)} = 0.25, \quad (8)$$

where $\alpha_{\mathrm{OPA}} = 0.764\ \mathrm{W}^{-1}$. At the same time, the expected squeezing and anti-squeezing levels were given by

$$R_- = 1 - \eta_{\mathrm{eff}} + \eta_{\mathrm{eff}}\, \mathrm{e}^{-2R} = -0.35\ \mathrm{dB}, \quad (9)$$

$$R_+ = 1 - \eta_{\mathrm{eff}} + \eta_{\mathrm{eff}}\, \mathrm{e}^{2R} = 0.46\ \mathrm{dB}. \quad (10)$$

Here, the total efficiency was $\eta_{\mathrm{eff}} = 0.18$, where

$$\eta_{\mathrm{eff}} = \eta_{\mathrm{OPA,in}} \eta_{\mathrm{OPA,out}} \eta_{\mathrm{OPA,prop}} \eta_{\mathrm{WDM}} \eta_{\mathrm{cables}} \eta_{\mathrm{BS}} \eta_{\mathrm{PD}}. \quad (11)$$

We used the following efficiencies to calculate η_{eff}: $\eta_{\text{OPA,out}} = 0.60$, $\eta_{\text{OPA,prop}} = 0.90$, $\eta_{\text{WDM}} = 0.77$, $\eta_{\text{cables}} = 0.83$, $\eta_{\text{BS}} = 0.95$, $\eta_{\text{PD}} = 0.80$, $\eta_{\text{OPA,in}} = 0.50$. From Eqs. (9) and (10), the expected levels of squeezing and anti-squeezing differed from the experimental results. Loss and phase noise are two common reasons for the mismatch between theoretical and experiment squeezing levels [7]. Losses degrade squeezing by introducing additional noise. Similarly, phase noise arises from an imperfect phase match between the LO and the squeezed light phase [11]. Another challenge is shaping the LO's spatial and temporal profiles to match the distorted squeezed light caused by gain-induced diffraction (GID) in nonlinear crystals [12]. Several sources could produce this disagreement between expected and experimental results, so further investigation is required to identify the cause.

5. Conclusions

The first measurement showed a mean fundamental optical power recorded was $588.08 \pm 4.13\ \text{mW}$, followed by an experimental analysis of the relation between the temperature and the power mean. The experiment led to the recording of an optimal phase matching temperature of $T_0 \sim 40.54\ °\text{C}$ with an experimental SHG power of $P_{\text{SHG}} \sim 81.53 \pm 0.16\ \text{mW}$. Finally, the squeezing and anti-squeezing levels were measured, with a dominance of anti-squeezing effects. The maximum anti-squeezing measured was $0.28\,\text{dB}$, while the maximum squeezing measured corresponded to $0.21\ \text{dB}$.

However, it is important to mention the discrepancy between the expected levels of squeezing and anti-squeezing compared to the experimental outcomes. Two typical effects that limit the usable squeezing are loss and phase noise, but further study is needed to identify the source of such discrepancy.

References

[1] Yan, Z.-H. *et al.* Generation of non-classical states of light and their application in deterministic quantum teleportation. *Fundamental Research* **1**, 43–49 (2021).

[2] Barsotti, L., Harms, J. & Schnabel, R. Squeezed vacuum states of light for gravitational wave detectors. *Reports on Progress in Physics* **82**, 016905 (2018).

[3] Lawrie, B. J., Lett, P. D., Marino, A. M. & Pooser, R. C. Quantum Sensing with Squeezed Light. *ACS Photonics* **6**, 1307–1318 (2019).

[4] Wang, Z. *et al.* Structured light analogy of quantum squeezed states. *Light: Science & Applications* **13**, 2, 12 (2024).

[5] Boyd, R. W. *Wave-Equation Description of Nonlinear Optical Interactions*, 1–135 (Elsevier, 2020).

[6] Choudhary, S. & Boyd, R. W. Tutorial on nonlinear optics. *Proceedings of the International School of Physics "Enrico Fermi"* **190**, 31–76 (2016).

[7] Adya, V., Karlsson, H. & Svanberg, E. Squeezing Lab Manual (2024).

[8] Jiang, Z. *et al.* Mitigating Scattering in a Quantum System Using Only an Integrating Sphere. *PRX Quantum* **5**, 030351–1, 030351–7 (2024).

[9] Merchant, F. A. & Periasamy, A. *Multispectral Fluorescence Imaging*, 201–245 (Elsevier, 2023).

[10] Jia, X., Wei, Q., Zhu, Y. & Zhang, W. Analysis of noise and its characteristics in avalanche photodiode. *AIP Advances* **14**, 1–6 (2024).

[11] Frascella, G., Agne, S., Khalili, F. Y. & Chekhova, M. V. Overcoming detection loss and noise in squeezing-based optical sensing. *npj Quantum Information* **7**, 1–2 (2021).

[12] Kashiwazaki, T. *et al.* Continuous-wave 6-db-squeezed light with 2.5-THz-bandwidth from single-mode PPLN waveguide. *APL Photonics* **5**, 1–2 (2020).